2

Electronically Reconfigurable Antenna with Switchable Beams

This chapter presents the design of a 2 x 1 reconfigurable beam steering array for WLAN applications. A simple and cost-effective technique is utilized to implement the concept of reconfigurability by applying the phase difference between the two elements of the antenna array using the RF PIN diodes. A demonstration antenna is simulated, fabricated, and measured to verify the proposed concept. This antenna array is designed on an FR4 substrate in which the two elements are fed through a microstrip line. The measured results indicate that the proposed antenna can steer its radiation pattern between -36° to +36° with respect to the antenna broadside within the overlapping bandwidth from 5.12 GHz to 5.41 GHz covering the WLAN frequency band from 5.15 GHz to 5.35 GHz. The simulated and measured results are found in good agreement. The advantage of the proposed design is that it provides a larger steering angle using the same profile as other references with minimal design complexities due to its planar structure.

2.1 Introduction

In modern wireless applications, adaptable or multifunctional antennas are demanding to fulfil the user requirements. This can be achieved by reconfigurable technology. The reconfigurable technology has been investigated in the modern antenna field. There are various techniques reported in the literature through which reconfigurability can be achieved, which include the use of PIN diode switches [92]-[93], varactor diodes [94], MEMS Switches [95], and tunable electromagnetic materials such as graphene, Liquid crystal (LC), and ferroelectric film [96]. The antenna with pattern reconfigurability can enhance the system security [97], channel capacity, and energy efficiency by pointing its signals towards the intended directions while suppressing the interference towards the unintended directions [98]. The pattern reconfigurability can be considered in three different categories. In the first category, the main beam of the antenna radiation pattern is reconfigured between the boresight and conical [99]-[100], which can enhance the link quality or the system quality. The second is to change the position of the pattern null [101]-[102], which can minimize the effects of interference in the radio environment. The third category includes the reconfigurable antennas, which can rotate its beam in different directions or prevent its beam from rotating. This property can save energy by directing the signals towards the intended users or providing a larger coverage area. Classically, beam steering can be achieved by using phased array systems [103]. In [104], a wide beam scanning angle from -81° to +81° is achieved using eight pattern reconfigurable antennas that can switch its radiation pattern between quasi-broadside to monopole-like pattern. A reconfigurable antenna is designed in [105] using electromagnetic bandgap (EBG) for dual-band operation at 2.45 and 5.8 GHz with a beam shifting at ± 26° from its broadside direction. In [106], two operational modes can be realized as omnidirectional and directional and a beam scanning of 360° was achieved in the directional mode by using the arc-shaped dipoles and a circular ring reflector. This antenna was fed by an external feeding

circuit which requires power dividers, attenuators, and phase shifters. The above designs provided the wide-angle of scanning, but simultaneously, they suffered from the drawback of large profile and high cost due to the requirement of external feeding networks and phase shifters. One more design using one rectangular antenna combined with one mushroom type EBG structure and one triple slotted EBG was studied in [107]. This antenna steered its beam from -20° to +20° in E plane and -18° to +18° in H plane for mushroom type EBG and triple slotted EBG from -18° to +18° in E plane and -15° to +15° in H plane. In [108], a beam tilt of +25° and -24° was achieved by using an adjacent square shaped metamaterial structure on the dipole antenna. A bent dipole antenna with a metal reflector was studied in [109] and a maximum beam tilt of ±48° was achieved by varying the distance between the dipole and metal reflector. However, it requires some mechanical arrangement to change the distance between the dipole and reflector which increased system complexity. In [110], the beam scanning of -32° to +36° was achieved using the microstrip Yagi antenna, varactor-loaded parasitic elements, and two orthogonal feeds to realize the circularly polarized (CP) beams. A two-element array with stub-loaded varactors was proposed to achieve a beam scanning of -23° to +23° with a frequency tuning from 2.15 to 2.38 GHz [111]. In [112], a Yagi antenna based on a microstrip patch was proposed to scan its beam from -40° to +40° by switching the varactor-loaded parasitic patches as reflectors or directors. But for these designs, continuously tunable varactor diodes were used to achieve continuous scanning, which requires a large series RF resistance to limit the DC current for biasing that decreases the system's overall efficiency and the use of parasitic element increases the overall dimensions of the antenna. In [113], an SP3T RF switch was used to select the two branches and by applying a phase difference between the two elements, the pattern was steered between -30° to +30° with an interval of 30°. In [114], a reconfigurable antenna was designed to steer its beam within -6 dB impedance bandwidth from 2.37 to 2.5 GHz for wireless headset application using a U-slot patch antenna.

In this chapter, a tunable phase-shifting mechanism is proposed by a reconfigurable feeding network (RFN) loaded with PIN diodes and an array of two patches. Each diode is turned ON or OFF separately by using an externally designed switching circuit that consists of single pole double throw (SPDT) switches and push to ON/OFF buttons and LEDs (red and green) to indicate the positive or negative biasing on the terminals V_1-V_{12}. This antenna achieved desired performance without using phase shifters, a complex beam-forming network, a large antenna footprint, and minimal design complexities compared with other existing literature. The antenna has applications in the wireless communication service band and WLAN systems. The design of pattern reconfigurable antenna, its biasing network, and derived electrical equivalent circuit are given in the following sections.

2.2 Design of Beam Steerable Antenna Array

2.2.1 Two Element Antenna Array Design

The objective of this section is to design a two-element antenna array. This array is designed at three stages, namely Ant-A, Ant-B, and Ant-C. A single patch antenna (Ant-A) is designed at the first stage. The antenna consists of a patch, quarter-wave transformer, and feedline (Fig. 2.1(a)). The antenna is printed on the FR4 substrate having a dielectric constant of 4.4 and thickness of 1.6 mm. The dimensions of the rectangular patch (Lp = 13.5 mm and Wp = 19 mm) are calculated using a standard design equation as given in [126] to achieve the resonance frequency of 5.15 GHz. A quarter-wave transformer is used to match the input impedance of the antenna to the 50-ohm transmission line. The same antenna is used to design the two-element array without any power divider (Ant-B) at the second stage. The two antennas are fed by individual ports, as shown in Fig. 2.1(b). At the third stage, a two-element array (Ant-C) with a power divider is studied in Fig. 2.1(c). It is essential to mention that patch dimensions remain the same in all three stages. The reflection coefficient for all stages are shown in Fig. 2.1(d). To achieve pattern

reconfigurability, a tunable phase shifter in terms of delay lines and PIN diodes are introduced in the feeding network. The detailed study is given in the following section.

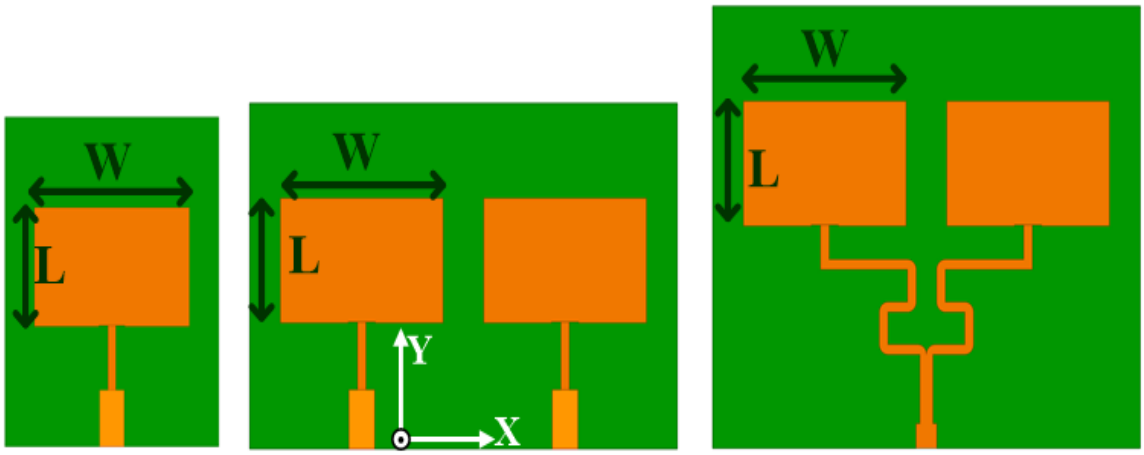

(a) (b) (c)

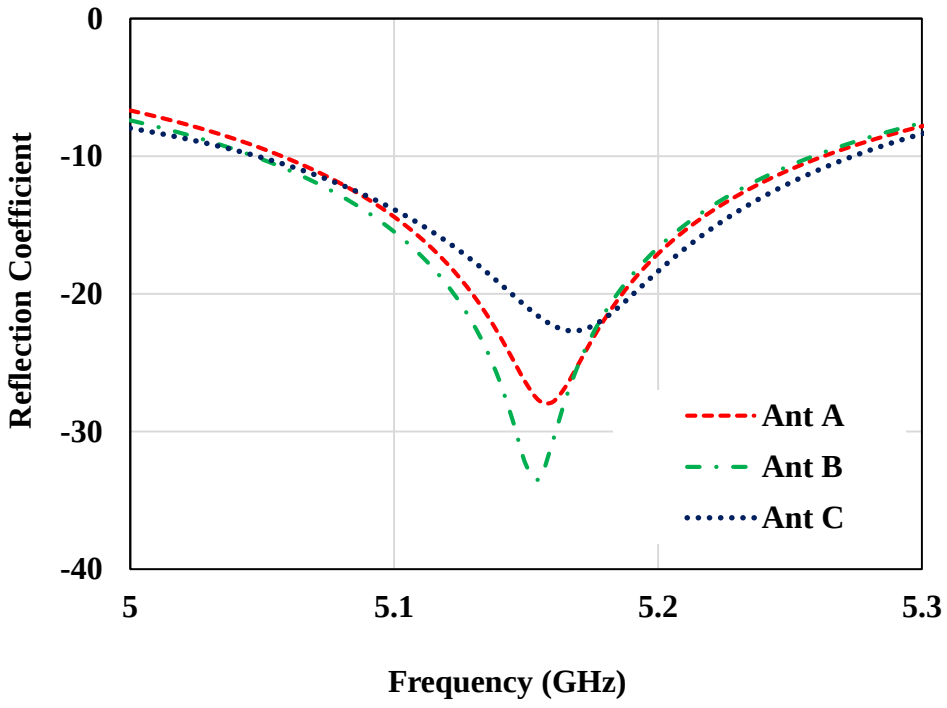

(d)

Figure 2.1: The design process of two-element antenna array. (a) Ant-A, (b) Ant-B, (c) Ant-C, and (d) Reflection coefficient of Ant-A, Ant-B and Ant-C.

2.2.2 Reconfigurable Antenna Array design

This section presents the detailed design of the reconfigurable two-element array with the beam steering mechanism. According to the array theory, the resultant pattern of an array can be steered by introducing the progressive relative phase difference between the antenna array elements. From Eqn. 2.1, when the phase difference (β) between the two elements is zero, the direction of the main beam is θ = 0°, i.e., the main beam direction will be broadside [116].

$$\beta = kd\sin\theta \qquad (2.1)$$

where k = phase constant (k = $2\pi/\lambda$) and d = inter-element spacing.

The directional array consists of two patch elements with an inter-element spacing of d = $0.40\lambda_0$, a metallic ground plane, printed on the backside of the substrate, and a reconfigurable feeding network. The feeding network consists of a 50-ohm transmission line (T_1), two 100-ohm transmission lines (T_2 and T_3), and a quarter-wave transformer used to match the

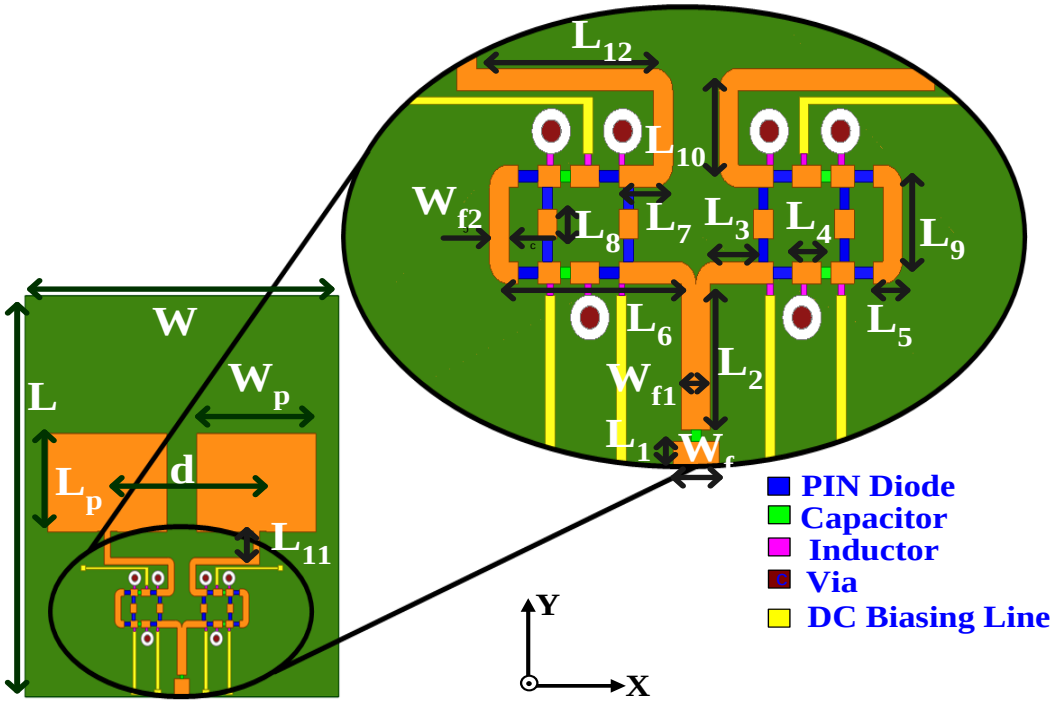

Figure 2.2. The geometry of two elements reconfigurable antenna array.

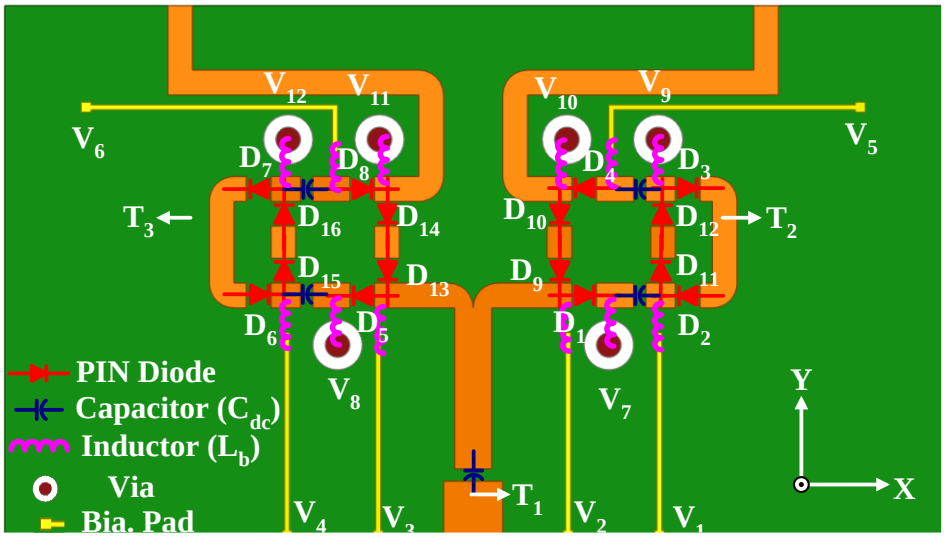

Figure 2.3: Reconfigurable feeding network with DC biasing circuit.

impedance of the 50-ohm transmission line to the 100-ohm transmission line. This array is printed on the FR4 substrate having a dielectric constant of 4.4 and thickness of 1.6 mm, as shown in Fig. 2.2. On the 100-ohm feed line, 16 RF PIN diodes are incorporated to achieve reconfigurability in the radiation pattern. The zoom-in view of the reconfigurable feeding network is shown in Fig. 2.3. The optimized dimensions of the proposed antenna are given in Table 2.1.

2.2.3 PIN Diode Equivalent Circuit Model

The RF PIN diodes are loaded on the feeding network to realize pattern reconfigurability. By switching the states of the pin diodes, different excitation paths are selected to excite the two elements. The suitable arrangement of the PIN diode to choose the different excitation paths is shown in Fig. 2.3. The selected PIN diodes are from Infineon Technologies with model no Bar64-02V and SC79 surface-mount packaging [124]. These diodes operate below 6 GHz with excellent switching performance. The equivalent circuit model of the RF switches incorporating the DC blocking capacitors (*C*) and the RF chokes (*L*) is shown in Fig. 2.4(a) The DC blocking capacitors prevent the biasing current from flowing through the RF port. The inductors provide the path for the DC current while

Table 2.1: **Optimized dimensions of the proposed beam steering antenna**

Parameter	Value (mm)	Parameter	Value (mm)	Parameter	Value (mm)
W	50	W_{f2}	1	L_6	9.95
L	55	L_1	2.5	L_7	2.8
W_P	19	L_2	6.5	L_8	1.3
L_P	13.5	L_3	3.25	L_9	5.3
W_f	2.4	L_4	1.5	L_{10}	3.3
W_{f1}	1.4	L_5	1.5	L_{11}	3.7

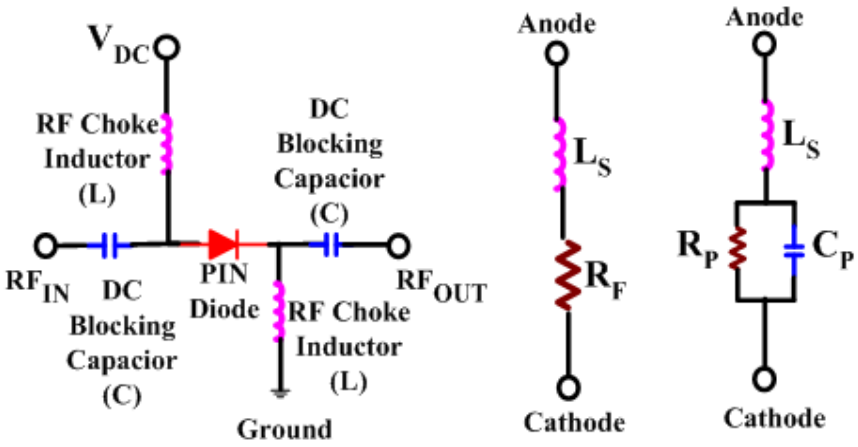

(a) (b) (c)

Figure 2.4: (a) The equivalent circuit of RF Switches consist of DC blocking capacitors and RF chokes (b) ON state of PIN diode and (c) OFF state of PIN diode.

barricading the RF current. The value of *L* and *C* are optimized equally as 15 nH and 6.2 pF, respectively.

The PIN diode can work in two operational modes: ON and OFF. According to the datasheet, when diode is ON, forward voltage of 0.82 V drops across the diode and a forward current of 10 mA flows through the diode. While using a diode in the OFF state works in reverse bias. The ON state of the PIN diode in simulation is modelled as a series combination of 2.4 Ω resistance (R_F), 0.6nH inductance (L_S) [124]. The OFF state is modelled as a series combination of 0.6 nH inductor (L_S) and a parallel combination of a

3.9 kΩ resistance (R_P) and a 0.13 pF capacitor (C_P=0.13pF) [124]. The equivalent circuit of the ON and OFF mode of the PIN diode is shown in Fig. 2.4 (b) and (c), respectively. The total maximum power consumed by the diode as calculated from the datasheet is 21 mW, i.e., P_{dc}= I_{dc}^2R= $(100mA)^2 \times 2.1\Omega$.

2.2.4 Switching Mechanism

The different radiation modes are obtained by applying the 12 different biasing voltages to the node V_1-V_{12}. The effect of the DC line on the radiation patterns is minimized by 0.2 mm wide DC isolation strips are used to connect the nodes V_1-V_6. The rest of the nodes, i.e., V_7-V_{12}, are connected to the ground plane through vias. When two elements are excited in the same phase through diodes D_9, D_{10}, D_{13}, and D_{14}, the broadside beam is realized as S_1. When the diodes D_9, D_{10}, D_5, D_{15}, D_{16} and D_{14} are turned ON and rest are in OFF state (S_2), an additional delay line of length 10.3 mm (0.175 λ_0) is added because the current travels an additional distance leading to path difference, which further produces a phase difference. This phase difference provides a beam tilt of -26° from Eqn. 2.1 in the radiation pattern from the broadside direction. Similarly, when the diode D_9, D_{10}, D_5, D_6, D_7 and D_8 are turned on (S_3), a beam tilt of -36° is observed. Since the antenna has symmetry, the S_4 and S_5 will be similar to S_2 and S_3. Table 2.2 represents the five different reconfigurable states and their reconfigured pattern characteristics and rest of the diode combination are not considered here due to its poor impedance matching. Since the reconfigurable feeding network is symmetrical about the X-axis, symmetrical tilting beam is obtained by swapping the states of the diodes about the X-axis. And hence the main beam direction varies from θ = -36° to +36°.

2.2.5 DC Biasing Circuit

The pattern reconfigurability is achieved by using 16 PIN diodes, as shown in Fig. 2.3. Practically, it is challenging to design 16 biasing circuits for these diodes. Hence, here we

have proposed a simple biasing circuit that requires only six DC voltages (only two DC voltages at a time, one for the left arm and one for the right arm) to control the operating states of the 16 PIN diodes. Table 2.3 presents the connection of the node voltages to the battery's positive and negative (GND) terminal for all realized modes.

Table 2.2: **PIN diode biasing conditions for different states**

	Diodes states		
State	**Forward biased**	**Reverse biased**	**Beam direction**
S_1	D_9, D_{10}, D_{13}, D_{14}	D_1-D_8, D_{11}, D_{12}, D_{15}, D_{16}	0°
S_2	D_9, D_{10}, D_5, D_{15}, D_{16}, D_8	D_1-D_4, D_6,D_7 D_{11}-D_{14},	-26°
S_3	D_9, D_{10}, D_5, D_6, D_7, D_8	D_1-D_4, D_{11}-D_{16}	-36°
S_4	D_{13}, D_{14}, D_1, D_{11}, D_{12}, D_4	D_2, D_3, D_5-D_{10}, D_{13}, D_{15}, D_{16}	+26°
S_5	D_{13}, D_{14}, D_1, D_2, D_3, D_4	D_5-D_{12}, D_{15}, D_{16}	+36°

Table 2.3: **DC node voltages for all states**

Node Voltage	**S_1**	**S_2**	**S_3**	**S_4**	**S_5**
V_1	OC	OC	OC	+Ve	GND
V_2	GND	GND	GND	+Ve	+Ve
V_3	GND	+Ve	+Ve	GND	GND
V_4	OC	+Ve	GND	OC	OC
V_5	OC	OC	OC	+Ve	+Ve
V_6	OC	+Ve	+Ve	OC	OC
V_7	OC	OC	OC	GND	GND
V_8	OC	GND	GND	OC	OC
V_9	OC	OC	OC	GND	+Ve
V_{10}	+Ve	+Ve	+Ve	GND	GND
V_{11}	+Ve	GND	GND	+Ve	+Ve
V_{12}	OC	GND	+Ve	OC	OC

OC- open circuit, GND- ground

2.3 Results and Discussion

The simulation of the proposed antenna is carried out using EM full-wave simulator HFSS version 18.2 [126]. For biasing of the diodes, DC wires carrying the bias are soldered on the DC pad. An SMA connector of 50 ohms is used to measure the reflection coefficient and pattern characteristics. The fabricated antenna, the reconfigurable feeding network, and an external switching circuit with soldering wires are shown in Fig. 2.5.

The reflection coefficient of the antenna is measured using Anritsu's VNA Master MS2038C by applying the different combinations of the switches. The simulated and measured resonances of the various combinations of the switches are shown in Fig. 2.6. For all realized states, the measured overlapped impedance bandwidth ranges between 5.12 GHz to 5.4 GHz with a reflection coefficient of less than -6 dB [112].

A slight difference is observed between simulated and measured results due to the fabrication tolerances. An approximate equivalent circuit used from the datasheet to model the PIN diodes in simulations is not that accurate to model the exact behaviour of diodes in real. Change in the

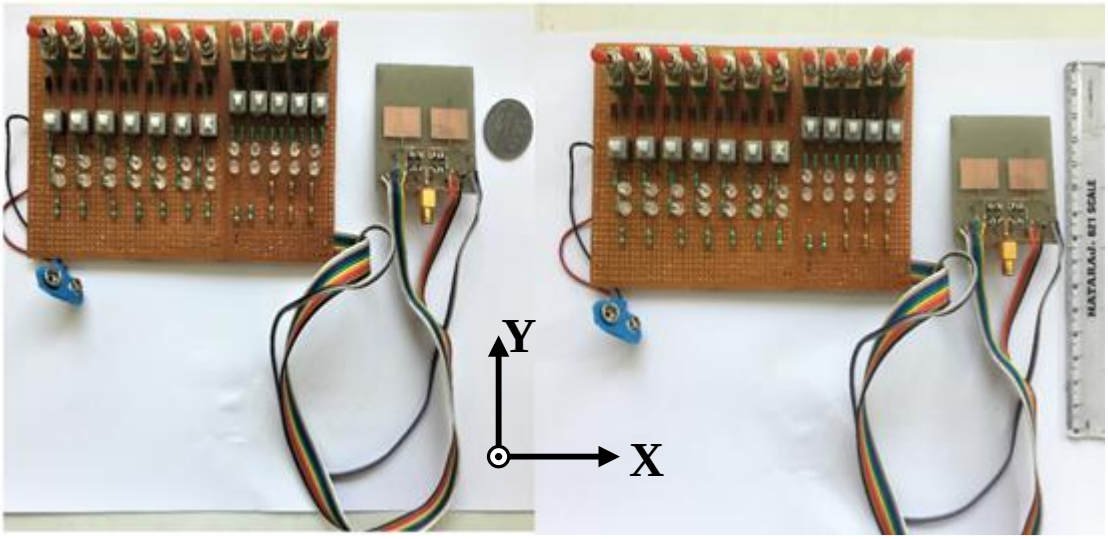

Figure 2.5: Fabricated view of the proposed antenna along with the switching circuit.

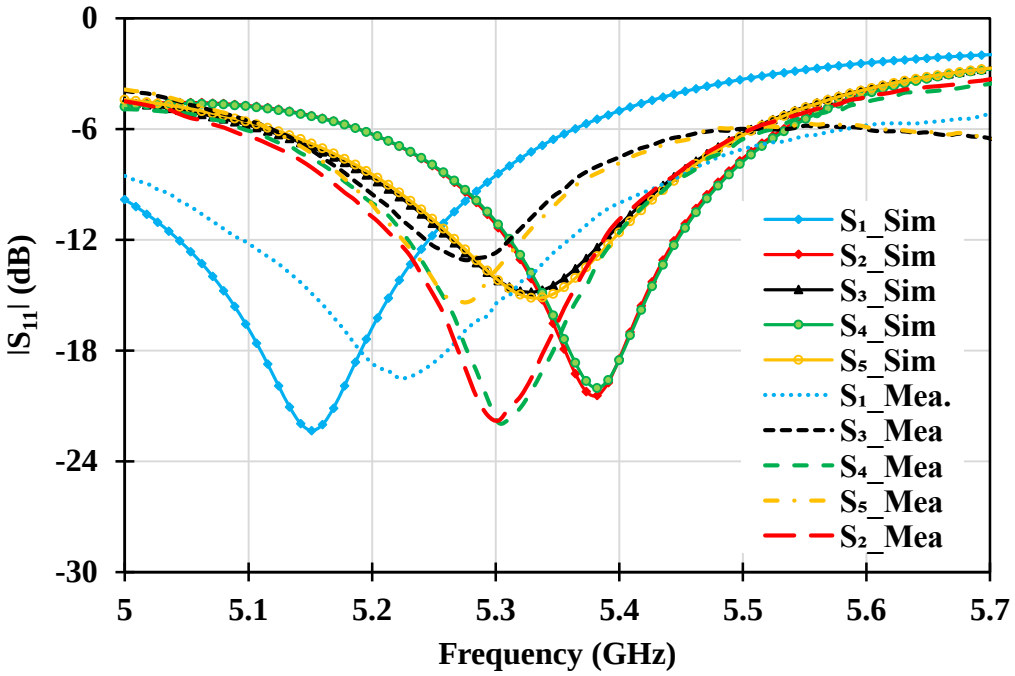

Figure 2.6: Simulated and measured reflection coefficient for all states.

material dielectric constant is also a concern [119]. Since the soldering of the diodes can not be made precisely identical, this will also affect the symmetrical properties of the antenna.

A far-field antenna measurement system is used to characterize the antenna. The proposed antenna was used as the receiving antenna, while an 800 MHz - 18 GHz standard double ridge horn antenna was used as the fixed transmitting antenna. A distance of 5.5 m separated the two antennas. During testing, bias lines along with the switching circuit were covered by a piece of the absorber to reduce its spurious radiation. The corresponding simulated and measured 2-D patterns in the XZ plane are shown in Fig. 2.7.

The different radiation patterns for all states are normalized with respect to the maximum value. A difference between simulated and measured radiation patterns is observed due to the external DC source and external switching network used to supply power for PIN diodes.

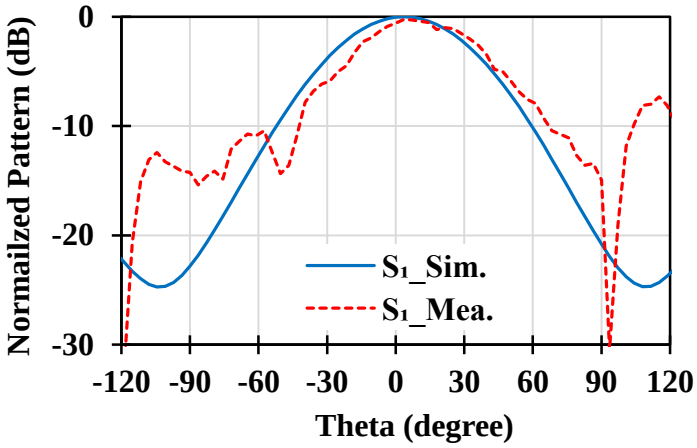

(a)

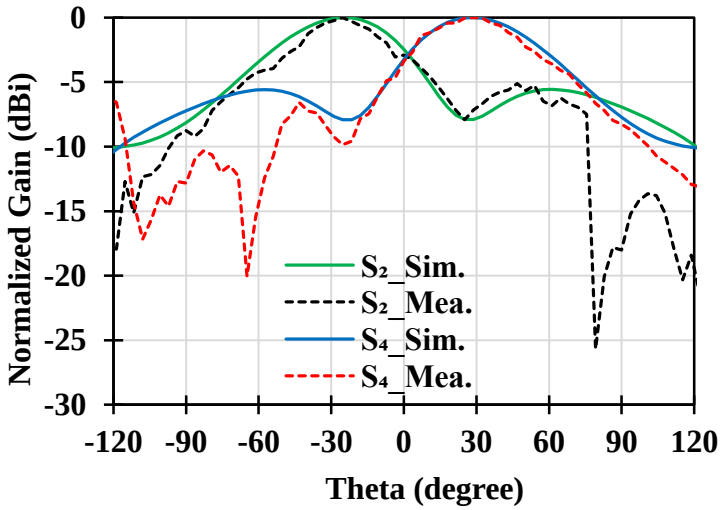

(b)

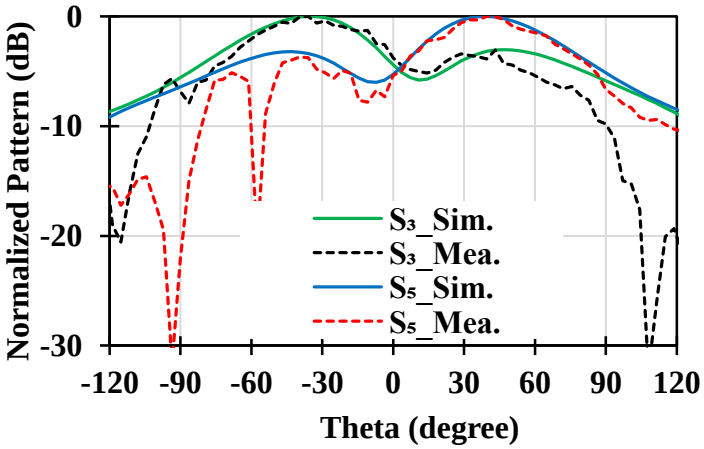

(c)

Figure 2.7: Simulated and measured radiation patterns in the XZ plane for states. (a) S_1, (b) S_2, S_4 and (c) S_3, S_5.

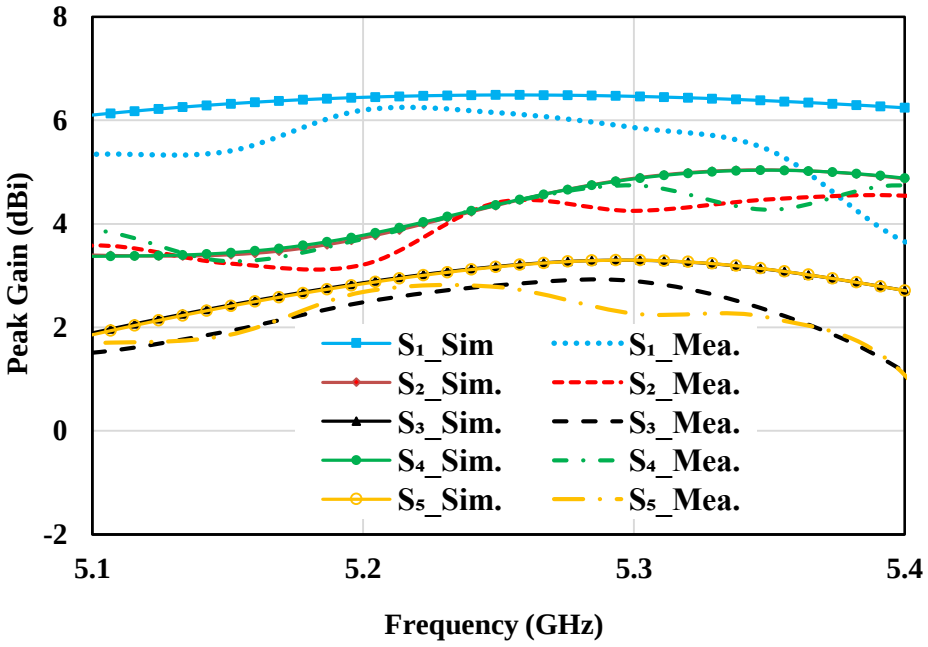

Figure 2.8: Simulated and measured gain for all states.

Also, the placement of PIN diodes and the biasing circuit on the radiation layer severely affects the antenna radiation property, as mentioned in [91]. It is observed that the main beam of the antenna is steering between -36° to +36° in the elevation plane (XZ) for different operating states.

The simulated and measured gain for all modes is summarized in Fig. 2.8. A certain difference is noticed between the simulated and measured results due to the inaccurate actual losses of the antenna circuit elements. The measured gain varies between 6.5 dB to 1.5 dB for all states within the operating band from 5.12 GHz to 5.4 GHz.

2.4 Comparison and Review

Table 2.3 refers to the comparison of the proposed antenna with some of the recently similar reported antennas. Antenna is comparable with other antennas in terms of dimensions, number of actuator used, number of reconfigurable modes, maximum beam tilt, and type of antenna configuration. Most of the antennas in Table 2.4 have either a multilayer structure or having the larger profiles with smaller steering angle as compared to proposed

antenna except antenna in ref. [111]. Although, the antenna presented in [111] has a larger steering angle but its profile is also larger than the proposed antenna. Therefore, the proposed antenna has the largest scanning angle with compact dimensions and is easy to fabricate because of its single-layer configuration. With this beam steering feature, this proposed antenna shows the potential for WLAN applications to cover the wider communication area without compromising the other aspects.

Table 2.4: **Comparison of the proposed beam steering antenna with the similar antenna**

Ref.	A	RM	MBT (°)	ST	TC	D (λ_g)
[105]	14 PD	3	±25, 0	discrete	multilayer	1.93x1.93x0.16
[107]	4 PD	4	0, ±20	discrete	Single with complex EBG	2.87x3.0x0.17
[108]	MM	2	+25, -24	discrete	Single with large dimension	1.63x2.20x0.02
[111]	4 VD	NA	±40	continuous	Single with very large profile	2.40x1.37x0.02
[112]	2 VD	NA	±23	continuous.	Single-layer	1.69×1.79×0.01
[115]	30 PD	3	±26	discrete	Multi-layer	1.97×1.57×0.49
[116]	8 PD	3	0, ±25	discrete	Multi-layer	1.47×1.81×0.49
[117]	PS	4	-6, -28, +9, +26	discrete	Multilayer	5.24×5.24×0.93
[120]	2 PD	3	0, ±30	discrete	Single with AMC	3.07×1.46×0.10
Pro. Work	16 PD	5	0, ±26, ±36	discrete	Single Layer	1.84×2.02×0.05

Here λ_g = guided wavelength at the center frequency, A = actuators, RM = reconfigurable modes, MBT = maximum beam tilt, ST = sacnning type, TC = type of configuration, D = dimension, MM = metamaterial, PS = phase shifters

2.5 Summary

A beam steering antenna with a reconfigurable feeding network for WLAN applications is presented in this chapter. The design methodology and detailed analysis are presented in detail for better understanding the working mechanism. To implement the reconfigurability

principle, sixteen PIN diodes are used on the phase shift feed network to control the phase difference between the two array elements and control the direction of the radiation pattern. Since the proposed antenna can produce five types of phase differences, hence it can have five types of reconfigurable beams oriented at 0°, ±26°, and ±36° within the overlapping bandwidth from 5.12 GHz to 5.41 GHz. The simulated and measured results are in close agreement, demonstrating the proposed concept's correctness.

In this chapter, a reconfigurable antenna with a single reconfigurable characteristic is studied, where some deterioration in the antenna radiation characteristics is observed due to the placement of the switching components and the biasing circuit on the radiation layer.

Therefore, in the next chapter, a wideband hybrid reconfigurable antenna with circular polarization reconfigurability is studied. Further, to minimize the effect of the switching components and biasing circuits on the antenna radiation, the feed network with all the active elements and biasing is placed as a separate layer.